Nitrogen availability facilitates phosphorus acquisition by bloom-forming cyanobacteria

Luis Aubriot*

Grupo de Ecología y Fisiología de Fitoplancton, Sección Limnología, Instituto de Ecología y Ciencias Ambientales, Facultad de Ciencias, UdelaR

*Corresponding author: Sección Limnología, Facultad de Ciencias, Universidad de la República, Iguá 4225, CP11400, Montevideo, Uruguay. Tel: +598-25258618, ext. 7148; Fax: +598-25258617; E-mail: laubriot@fcien.edu.uy

One sentence summary: Nitrogen availability facilitates phosphorus acquisition by the activation of high-affinity phosphate uptake systems of N-deficient cyanobacteria during the onset of bloom formation

ABSTRACT

Cyanobacterial blooms are threatening freshwater ecosystems. The physiological basis involved in the onset of cyanobacterial bloom is fundamental to advance in bloom predictions. Generally, cyanobacteria grow until the availability of nitrogen (N), phosphorus (P) or both nutrients becomes limited. Population survival may depend on physiological adjustments to nutrient deficiency as well as on the efficient use of episodic N and P inputs. This study investigated the effect of N inputs on phosphate uptake affinity and activity of N-deficient bloom-forming cyanobacteria. Lake samples dominated by filamentous cyanobacteria were preincubated with and without nitrate addition, and the uptake of [^{32}P] phosphate pulses was measured in the following days. Phosphate uptake kinetics were analyzed with a flow-force model that provides the threshold concentration, reflecting phosphate uptake affinity, and the membrane conductivity coefficient that corresponds to the activity of uptake systems. After 24 h of nitrate preincubation, phosphate uptake kinetics showed a progressive increase in affinity (nanomolar $[P_e]_A$) and activity (25-fold) concomitant with cyanobacterial growth. It was demonstrated that the alleviation of N-deficiency by N inputs boosts the activation of phosphate uptake systems of non-N_2-fixing cyanobacteria to sustain growth. Therefore, reduction of dissolved inorganic N levels in lakes is also mandatory to limit cyanobacterial phosphate uptake affinity and activity capabilities.

Keywords: cyanobacterial blooms; nutrient colimitation; nutrient deficiency; physiological regulation; phosphate uptake; eutrophication

INTRODUCTION

Eutrophication and cyanobacterial blooms in lakes are threatening the conservation of freshwater resources, biodiversity and human health (Dokulil and Teubner 2000; Schindler *et al.* 2008; Paerl 2018). Some factors causing bloom formation are well known, such as the effect of certain human activities that increase the concentration of phosphorus (P) and nitrogen (N) in lakes and catchments in combination with the effects of climate change (Smith and Schindler 2009; Dolman *et al.* 2012; Sinha, Michalak and Balaji 2017; Yan *et al.* 2017). However, phytoplankton often go through periods of nutrient deficiency, in which P-deficiency may fluctuate throughout the seasons, while N-limitation generally occurs in spring and summer, particularly in eutrophic lakes (Schindler 1977; Paerl *et al.* 2014; Chaffin *et al.* 2018). Thus, cyanobacteria are exceptionally resistant to environmental changes and are capable of persisting for long periods of N and P limitation, even after lake restoration (Schindler *et al.* 2008). In these cases, the control of cyanobacterial proliferation

generally requires physical and geochemical applications (Bormans, Maršálek and Jančula 2016; Lürling, Waajen and de Senerpont Domis 2016). When catchment nutrient loads decrease, the cyanobacterial biomass can be sustained by episodic diffusive nutrient flows from sediments and the atmosphere (Galloway *et al.* 2004; Xu *et al.* 2010; Roy *et al.* 2012). Some nutrient sources cannot be directly controlled by local lake management, such as the increasing atmospheric deposition of inorganic N in lakes and catchments (Galloway *et al.* 2004). Moreover, the atmospheric deposition of N has been found to modify the N:P stoichiometry of lakes and, therefore, to induce shifts in phytoplankton nutrient deficiency as well as bloom formation (Elser *et al.* 2009; Zhan *et al.* 2017). Information about the timescale of such shifts in nutrient deficiency and about how cyanobacteria may benefit from these nutrient fluctuations is fundamental to advances in realistic bloom predictions.

The ecophysiologial traits that promote cyanobacterial bloom formation and resilience under nutrient fluctuations are not clearly understood. Cyanobacteria, and presumably eukaryotic phytoplankton, are very flexible organisms that respond physiologically to short-term environmental fluctuations (Stomp *et al.* 2008; Aubriot, Bonilla and Falkner 2011). The time required for this response should match the timescale of the external fluctuation in order to be efficiently used by organisms (Stomp *et al.* 2008). The organism-environment interplay is even more complex considering that each physiological process requires specific reaction times, such as pigment differentiation (Stomp *et al.* 2008), nutrient acclimation (Scanlan *et al.* 1997; Pitt *et al.* 2010) and regulation of nutrient uptake kinetics (Falkner, Priewasser and Falkner 2006; Aubriot and Bonilla 2012). In particular, cyanobacteria are able to sense phosphate availability and respond to it by concatenated energetic and kinetic adjustments of the uptake systems within minutes (Aubriot, Bonilla and Falkner 2011) followed by the reconstruction of the functional organization of the membrane P-binding proteins within hours or days, such as during phosphate starvation (Orchard, Webb and Dyhrman 2009; Pitt *et al.* 2010; Wu *et al.* 2012). During this process, the high-affinity phosphate uptake systems are progressively activated until the external nutrient attains a nanomolar threshold value due to the energetic restrictions (Falkner, Falkner and Schwab 1989). When P-deficient cyanobacterial populations are exposed to phosphate pulses over several minutes, the regulation of phosphate uptake activity takes place by decelerating uptake velocity, which occurs long before exhausting their P storage capacity (Aubriot and Bonilla 2012). Longer term deceleration of phosphate uptake rates also takes place when populations become N-limited (Aubriot and Bonilla 2018). In this case, active phosphate uptake may be re-established when growth is triggered after pulses of N supply, for example, during rainfall over an N-fertilized catchment or N solubilization through atmospheric N inputs.

Recently, it has been shown that fluctuations in N:P ratios are related to the regulation of phosphate uptake systems by cyanobacteria-dominated phytoplankton (Aubriot and Bonilla 2018). Other studies have shown that N addition to a P-deficient N_2-fixing cyanobacterium (*Dolichospermum flos-aquae*) upregulates the genes involved in P-metabolism, thereby suggesting a mutual nutrient dependence (Wang *et al.* 2018). However, the capacity of non-N_2-fixing cyanobacterial populations to activate the phosphate uptake systems after shifting from N-deficiency to nutrient availability, and the timescale and magnitude of the process, remain undefined. The activation of nutrient uptake by cyanobacteria may be fundamental to match environmental nutrient fluctuations and, hence, to achieve growth optimization. Understanding such processes is crucial to dissect the ecophysiology of cyanobacterial populations before and during bloom formation. Additionally, it may help to explain the resilience capability of cyanobacteria after reduction of external nutrient loads.

This study deals with the effect of nutrient deficiency shifts, from N-limitation to the nutrient availability, on the activity and affinity of phosphate uptake systems of cyanobacteria-dominated phytoplankton. The timescale of this process is fundamental to learn how bloom-forming cyanobacteria are able to exploit changes in nutrient availability in order to optimize growth. Lake samples dominated by filamentous cyanobacteria were preincubated with and without nitrate addition, and the uptake of [^{32}P]-labeled phosphate pulses was measured during the following days to evaluate the resulting uptake kinetics. These results offer an insight into the physiological responses of cyanobacterial populations to concomitant short-term N and P fluctuations as well as into N and P dependence to sustain growth.

MATERIALS AND METHODS

Study area and *in situ* measurements

Samples were taken from Lago Rodó, a shallow and polymictic hypereutrophic urban lake in Montevideo (34°54'47.32'' S – 56°10'1.64'' W) with a mean depth of 1.5 m (max. depth: 2 m, area: 1.3 ha). For several years, the lake was supplied with groundwater containing high dissolved nutrient concentrations with extremely high dissolved inorganic N (DIN) to phosphate (SRP) ratios >300:1 (6.4 ± 0.6 μM total P, 2.2 ± 0.2 mM total N) (Aubriot, Wagner and Falkner 2000). This nutrient inflow sustained high biomass of P-deficient phytoplankton until the groundwater supply was permanently interrupted and a significant depletion of DIN was detected (Aubriot and Bonilla 2018). The experiments were performed during periods of high and low DIN:SRP ratios.

The water column was characterized by temperature, dissolved oxygen and pH measurements taken every 20 cm from the surface to the bottom by using Horiba OM−14 and D−24 sensors. A 5 L water sample was taken from the lake surface with a dark bottle, and transported to the laboratory within 30 min to conduct the experiments and chemical and biological analyses.

Spectrophotometric determinations

SRP and DIN (NO_3^-, NO_2^- and NH_4^+) concentrations were analyzed in the filtrate (GF/F Whatman glass fiber filters, presoaked in ultrapure water) using standard colorimetric methods (Strickland and Parsons 1972). Total P (TP) and total N (TN) were determined with the unfiltered sample (Valderrama 1981). Chlorophyll *a* (Chl *a*) was analyzed in triplicate samples according to Nusch (1980).

Phytoplankton composition and biovolume

An aliquot of 450 mL of the 5 L lake water sample was fixed with acid Lugol's solution and stored in darkness until processing (within three months). Identification to genus or species level was performed with organisms larger than 5 μm in diameter (Sant'Anna 1984; Wehr and Sheath 2003; Komárek and Anagnostidis 2005). Counting was performed in a 1 mL Sedgwick-Rafter chamber in random fields (Guillard 1978). Individual biovolume was calculated with geometric shapes and the average of linear dimensions (length, width and depth) of 10–30 organisms per

taxon (Hillebrand *et al.* 1999). The relative biovolume contribution of cyanobacteria was expressed as a percentage of the total phytoplankton biovolume (Cya %).

Theoretical considerations of phosphate uptake kinetics

The dependence of net uptake rates on the external phosphate concentration was analyzed with the flow-force model of Falkner, Falkner and Schwab (1989). The model gives two physiological parameters: the threshold value ($[P_e]_A$), a characteristic limiting phosphate concentration at which the incorporation of external phosphate by the cell is not energetically possible, therefore reflecting the affinity of the uptake systems; and the membrane conductivity coefficient (L_P), which is proportional to the maximum uptake (indicator of the activity of the uptake systems). The flow-force model was applied to studies investigating the variations of $[P_e]_A$ and L_P in response to nutrient fluctuations (e.g. Falkner and Falkner 1989; Falkner *et al.* 1995; Wagner, Falkner and Falkner 1995; Aubriot, Wagner and Falkner 2000; Aubriot and Bonilla 2018). On the other hand, the classical Michaelis-Menten single enzyme kinetic model has been used to analyze phytoplankton nutrient uptake; however, concerns have been raised regarding its correct application (Falkner *et al.* 1995; Bonachela, Raghib and Levin 2011; Aubriot and Bonilla 2018).

The flow-force model of Falkner (1989) is as follows:

$$J_P = -\mathrm{d}[P_e]/\mathrm{d}t = L_P\,(\log [P_e] - \log [P_e]_A) \quad (1)$$

where J_P is the uptake rate, expressed in the same units as L_P (μmol P [mg Chl *a* h]$^{-1}$), and $[P_e]$ is the external phosphate concentration. The plot of J_P versus log $[P_e]$ (Thellier plot, Thellier 1970) yields a straight line within the validity range of the model. The slope represents L_P and intercepts the log $[P_e]$ axis at the logarithmic $[P_e]_A$. The flow-force relationship is linear over a concentration range; however, linearity can be lost during kinetic and energetic regulation of cellular uptake systems (Thellier 1970; Falkner, Priewasser and Falkner 2006; Aubriot, Bonilla and Falkner 2011). Under such conditions, the uptake kinetics can be modeled by adding non-linear terms to equation (1) (Falkner, Priewasser and Falkner 2006), leading to

$$J_P = -\mathrm{d}[P_e]/\mathrm{d}t = L_P\,(\log [P_e] - \log[P_e]_A) + L(\log[P_e] - \log [P_e]_A)^m \quad (2)$$

where $m > 1$. Values of $m = 3$ or $m = 5$ were used to achieve a satisfactory fit ($r^2 \geq 0.9$) as described before (Aubriot, Bonilla and Falkner 2011). L is the conductivity coefficient of the non-linear term. The L results in values generally two orders of magnitude lower than L_P. A detailed theoretical explanation of the Falkner flow-force model is provided elsewhere (Falkner, Falkner and Schwab 1989; Falkner *et al.* 1995; Wagner, Falkner and Falkner 1995; Aubriot, Bonilla and Falkner 2011).

Measurement of phosphate uptake

Phosphate uptake was evaluated using ^{32}P-labeled phosphate applied to an aliquot of original lake samples. Subsamples were gently mixed with a magnetic stirrer and acclimated to 25 ± 1°C and illuminated at a saturating light intensity (150 μmol photons m^{-2} s^{-1}). Phosphate deficiency was characterized by using the P-deficiency index (PDI) (Lean and Pick 1981; Istvánovics *et al.* 1992) and also by describing the activity of phosphate uptake systems. The L_P values considered to express low activity of the uptake systems were within the 'no deficiency' PDI range (<1.1 μmol P_i [mg Chl *a* h]$^{-1}$). The L_P values over 1.1 μmol P_i (mg Chl *a* h)$^{-1}$ indicated moderate-to-high uptake activity.

Phosphate removal by organisms was measured with micromolar additions of [^{32}P] orthophosphoric acid (PerkinElmer, Waltham, MA, USA) in K_2HPO_4 (0.5–5 μM, leading to specific activities of 10–37 kBq μmol P^{-1}). Sample aliquots (0.8–1.5 mL) were filtered through Millipore (Darmstadt, Germany) HA filters (0.45 μm pore size) at time intervals of 0.5, 2, 5, 10, 15, 20, and 35 min, then every 30–60 min (as indicated in the figures) until reaching $[P_e]_A$ value. The net phosphate uptake integrates the nutrient removal by the dominant biomass of cyanobacteria with a small percentage of eukaryotes and bacterioplankton (<4% of the total phytoplankton biovolume, Sommaruga and Robarts 1997). The radioactivity in the filtrate was measured in 10 mL of ultrapure water using plastic vials and counted in a Beckman liquid scintillation counter (LS 6000, Beckman Coulter Inc., Brea, CA, USA) via Cherenkov radiation with a counting error of <5%. The calculated P_e concentration measured with $^{32}P_e$ was corrected according to the corresponding dilution of specific ^{32}P activity by the environmental SRP concentration as stated in Aubriot and Bonilla (2018). The correction of $[P_e]_n$ (at time n during the time course of $^{32}P_e$ removal) was calculated as:

$$[P_e]_n = {}^{32}P_{e\ n}\ [SRP] + {}^{32}P_{e\ ini} \,/\, {}^{32}P_{e\ ini} \quad (3)$$

where $[^{32}P_e]_n$ is the apparent phosphate concentration measured at time n in the time course of phosphate removal after the initial $[^{32}P_e]$ addition ($[^{32}P_e]_{ini}$), and SRP is the spectrophotometrically measured soluble reactive phosphorus. Since [^{32}P] phosphate was added after 20–24 h of nitrate addition (t_{inc}), the initial SRP (SRP_{ini}) had to be estimated when the lake SRP was detectable (see experiments C and D below), and in order to determine the $[P_e]_n$ (i.e. SRP plus [^{32}P] phosphate). Thus, the initial linear [^{32}P] uptake rate (first 30–60 min) ($L_{P\,lin}$, in μM [^{32}P] phosphate h^{-1}) was determined for each pulse addition in order to calculate the SRP_{ini} as:

$$SRP_{ini} = SRP - L_{P\,lin} \cdot t_{inc} \quad (4)$$

Positive SRP_{ini} values were obtained only in the SC subsamples (not preincubated with nitrate). When a negative SRP_{ini} was obtained, lake SRP was considered below detection limits, and therefore as a negligible concentration.

Experimental design

Four experiments (A–D) were performed during the summers of 2003, 2006 and 2007 with water samples from the Lago Rodó. Experiments A and B were designed to compare the [^{32}P] phosphate uptake kinetics during contrasting periods of DIN:SRP ratios. Experiments C and D were designed to show the effect of nitrate preincubation on [^{32}P] phosphate uptake kinetics of cyanobacteria-dominated phytoplankton. Experiment A was conducted during the period of groundwater supply into Lago Rodó, while experiments B, C and D were performed under interrupted water inflow (Aubriot and Bonilla 2018). All experiments were designed with a combination of phosphate pulses, defined in previous studies (Aubriot, Bonilla and Falkner 2011; Aubriot and Bonilla 2012). The applied [^{32}P] phosphate concentrations

were defined within the 'test pulse' range (<2 μM [^{32}P] phosphate; Aubriot and Bonilla 2012) in order to minimize effects on the regulation of phosphate uptake systems induced by the external concentrations (experiments A, B and C). In experiment D, the phosphate concentrations applied were slightly over the test range in order to induce adjustments in phosphate uptake kinetics (Aubriot and Bonilla 2012).

Experiment A consisted of two consecutive pulses of 1.0 μM [^{32}P] phosphate applied to subsample S1 (at times 0 and 169 min), while in experiment B two pulses of 1.2 μM [^{32}P] phosphate were applied (at times 0 and 245 min). In experiments C and D, subsamples S1 and S2 were preincubated with 250 μM nitrate, while subsample SC (control) was kept without nitrate addition. In experiment C, the phosphate uptake was evaluated by applying two phosphate pulses of 0.45 μM [^{32}P] to S1, and two pulses of 0.85 μM [^{32}P] to S2. The first pulses to S1 and S2 were applied at 20 h and the second ones at 39.17 h after nitrate addition (time zero). In order to evaluate the differences in uptake kinetics between S1 and S2, a third test pulse with the same concentration was added to each subsample (0.6 μM [^{32}P] phosphate) at 40.17 h after nitrate addition. In SC (control), only 0.45 μM [^{32}P] phosphate was added at 20 h and the time course of phosphate removal was followed during the following days. In experiment D, higher concentrations were used in order to test if cyanobacterial populations re-establish the phosphate uptake regulation capacity after activation of uptake systems (Aubriot and Bonilla 2012): two [^{32}P] phosphate pulses of 0.9 μM phosphate were applied to S1 and two pulses of 1.8 μM phosphate to S2 (at 24 and 47.92 h, first and second pulses, respectively). A third test pulse with the same concentration was added to S1 and S2 (2.4 μM [^{32}P] phosphate) at 49.08 h after nitrate addition. One pulse of 0.85 μM was added at 24 h to the control SC. In all experiments, the time course of [^{32}P] phosphate removal was followed until the attainment of $[P_e]_A$ value in order to fit the flow-force model. The second and third [^{32}P] phosphate pulses were applied only if the threshold value of the last pulse was attained.

Growth measurements

The same treatments used in [^{32}P] uptake experiments, with and without nitrate addition, were applied to temporary parallel replicates (S1, S2 and SC), through using non-radioactive K_2HPO_4 applied to 350 mL samples poured into 500 mL sterilized glass bottles. Three replicates were used as control SC (without nitrate addition), S1 and S2 with the application of 250 μM nitrate. Replicates were gently bubbled with humidified (Milli-Q water), prefiltered (GF/F sterilized) air. Light and temperature conditions were the same as those in the phosphate uptake experiments. The time course of biomass production was evaluated by measuring optical density (OD, absorbance at 750 nm) twice a day in a spectrophotometer (Beckman DU 600). Chl *a* concentration extracted with hot ethanol was determined at the beginning and end of incubations according to Nusch *et al.* (1980). Samples for phytoplankton analyses (taxonomic identification, counting and specific biovolume) were taken at the beginning and end of the experiments.

Growth rate (μ, d^{-1}) was calculated by integrating the biomass increase during four days using the equation:

$$\mu = (\ln OD_f - \ln OD_i)/(t_f - t_i)$$

Table 1. Physicochemical characterization of Lago Rodó . GWS: period of groundwater supply (+) and supply interruption (-); T: water temperature (surface-bottom); DO: dissolved oxygen (surface-bottom); SRP: soluble reactive phosphorus; TN: total nitrogen; TP: total phosphorus; DIN: dissolved inorganic nitrogen. *To estimate DIN:SRP when concentrations were below detection limits (DL), $\frac{1}{2}$ DL was used for calculation purposes.

Experiment	A	B	C	D
Date	4 February 2003	7 March 2006	4 January 2007	10 January 2007
GWS	+	–	–	–
T (°C)	25.0–24.8	25.0–25.0	27.5–26.3	25.2–25.0
DO (mg L^{-1})	9.6–5.7	7.9–5.5	12.6–3.7	8.0–3.0
NO_3^- (μM)	18.7	<3.6	<3.6	<3.6
NO_2^- (μM)	1.8	<0.2	<0.2	<0.2
NH_4^+ (μM)	1.3	4.2	10.5	5.6
SRP (μM)	<0.2	<0.2	2.4	2.5
TN (μM)	125.8	216.7	210.3	203.3
TP (μM)	5.3	6.1	9.3	8.5
TN:TP	23	35	23	24
DIN:SRP*	127	61	5	2

where t_f and t_i are the final and initial times, respectively. The average growth rates of the three replicates were calculated for each treatment.

Data analysis

The flow-force model of Falkner was run with MLAB (Mathematical Modeling System, Civilized Software, Inc., Silver Spring, MD, USA). Statistical differences in L_P between control and S1 or S2 treatments were performed first by data linearization according to Thellier (1970) and statistically analyzed with GLM-ANCOVA test. When variables fulfilled normality and constant variance, one-way analysis of variance (ANOVA) was conducted and the Holm-Sidak *post hoc* test was used for multiple comparisons. Statistical analyses were run with Statistica 8.0 (Stat-Soft, Inc., Palo Alto, CA, USA) and SigmaPlot 11.0 (Systat Software Inc., San Jose, CA, USA).

RESULTS

Lake conditions and phytoplankton composition

Surface lake temperature on the dates of the experiments ranged from 25.0–27.5° C, with mixed water columns except on one date (Table 1). Dissolved oxygen (DO) displayed marked differences between surface and bottom, particularly during summer 2007; nonetheless, anoxic conditions were not detected. During the period of groundwater interruption, nitrate and nitrite were below detection limits while ammonium concentration increased (Table 1). SRP was low on the dates of experiment A (<0.3 μM) and detectable during summer 2007 and without groundwater supply. No marked differences were detected in TP (mean: 7.3 ± 1.9 μM), TN (mean: 182.8 ± 38.8 μM) and TN:TP ratios (25.3 ± 3.9) among sampling dates. Differences were observed in DIN:SRP ratios, from high values during groundwater supply (DIN:SRP = 127) to lower ones during groundwater supply interruption (DIN:SRP = 2).

Phytoplankton was dominated by cyanobacteria (from 87–92% of total biovolume) on the dates of the experiments (Table 2). Chlorophyll *a* concentration in Lago Rodó ranged from 125.7–

Table 2. Main phytoplankton taxa, specific and total biovolume, relative cyanobacterial biovolume, chlorophyll *a* concentration in phytoplankton samples taken from Lago Rodó and used for experiments A–D. Mean values with standard deviation between brackets. Growth rates obtained from experiments C and D, SC, control, and S1 and S2 preincubated with nitrate. I: initial conditions of the corresponding experiment. See the applied [^{32}P] pulse additions in Table 3. Significantly different chlorophyll values are denoted with letters in lower case (without brackets) to compare lake conditions. Letters between brackets denote significant differences between treatments in each nitrate preincubation experiment (one-way ANOVA, Holm-Sidak *post hoc* test).

	Biovolume (mm^3 L^{-1})	Experiment									
		A	B	C				D			
				I	SC	S1	S2	I	SC	S1	S2
Cya	*Planktothrix agardhii*	4.01	6.77	6.39	4.40	26.91	28.39	4.86	3.02	12.33	17.83
Cya	*Raphidiopsis mediterranea*	0.46	0.04	0.40	0.41	2.77	1.68	7.00	7.37	5.18	7.59
Cya	*Microcystis* spp.	2.56						0.01	0.01		
Cya	*Anabaena* sp. and *Aphanizomenon* sp.									1.61	1.21
Cya	*cf. Limnothrix* and *cf. Planktolyngbya*	0.80	0.26							0.53	1.40
Cya	*Aphanocapsa cf. elachista*		0.49								
Bac	*Aulacoseira granulata*		0.19								
Bac	*Synedra* sp.	0.32		0.87	0.69	1.26	0.85	0.86	3.09	11.86	3.73
Bac	*Cyclotella* spp.	0.67				0.02	0.01				
Chl	*Scenedesmus* sp. and *Monoraphidium* sp.		0.12							0.25	0.10
Chl	*Selenastrum* sp.						0.68			2.40	
Chry	*Cryptophyta* spp.					0.80	0.25				2.50
Dino	*cf. Peridinium*		0.79	0.10	0.10			0.41			
	Total biovolume (mm^3 L^{-1})	8.50	8.66	7.8	5.6	31.76	31.86	13.14	13.49	34.16	34.36
	Chlorophyll *a* (μg L^{-1})	136.8 (11.9) a	125.9 (0.6) ab	125.7 (5.8) ab(a)	135.7 (7.0) (a)	296.0 (5.1) (b)	278.2 (14.8) (b)	147.5 (2.4) ac(a)	139.6 (10.1) (a)	308.3 (4.5) (b)	304.9 (14.6) (b)
	Relative biovolume Cya (%)	92	87	87	86	94	94	90	77	58	82
	Growth rate (d^{-1})				0.05 (0.01)	0.47 (0.01)	0.43 (0.02)		0 (0)	0.38 (0.02)	0.39 (0.01)

147.5 μg Chl *a* L^{-1} with significant differences between D (10 January 2007), and B and C (7 March 2006 and 4 January 2007, respectively) (ANOVA, $P = 0.012$, Holm-Sidak *post hoc* test, Table 2). Phytoplankton was dominated by cyanobacteria *Planktothrix agardhii* in samples of experiments A, B and C, and with co-dominance with *Raphidiopsis mediterranea* in experiment D. The BV of *Microcystis* spp. and the diatom *Synedra* sp. were also relevant in experiments A, and C and D, respectively (Table 2). The nitrate incubations applied in experiments C and D resulted in high chlorophyll *a* values (max.: 308.3 μg Chl *a* L^{-1}). Dominance of *P. agardhii* was observed in nitrate incubation treatments. Co-dominance of *P. agardhii* with *Synedra* sp. was detected only in S1 of experiment D.

Effect of lake conditions and nitrate preincubation on phosphate uptake kinetics

Experiments A and B were run during periods of groundwater supply and interruption, respectively (Fig. 1). Experiment A shows the characteristic features of active phosphate uptake systems as evaluated with the flow-force model (mean L_P = 11.8 μmol P_i [mg Chl *a* h]$^{-1}$; $[P_e]_A$ = 19 nM phosphate). Two consecutive pulses of 1 μM [^{32}P] phosphate were removed within 30 min until reaching nanomolar threshold values ($[P_e]_A$ = 15.2 nM, second pulse). In experiment B, the first pulse showed lower uptake rates than in A, with L_P and $[P_e]_A$ values close to the 'no deficiency' range (PDI <1.1 μmol P_i [mg Chl *a* h]$^{-1}$; $[P_e]_A$ = 62.9 nM, first pulse) (Table 3). The best fit of the time course of [^{32}P] phosphate removal of the second pulse was obtained with linear regression (Fig. 1B). The uptake rate dropped to 0.79 μmol P_i [mg Chl *a* h]$^{-1}$ and the threshold value was not attained during the incubation period. Similar linear trends of [^{32}P] phosphate removal and uptake rates were obtained in the control treatments (SC) of experiments C and D, although tested for an extended time period (up to 52 h) (see Figs 2 and 3, and Table 3).

Nitrate preincubation experiments allowed detection of the way in which phosphate uptake kinetics can be modified by DIN supply during a period of high SRP and low DIN concentrations (Tables 1 and 3). In experiment C, [^{32}P] phosphate uptake kinetics were measured after 20 h of nitrate preincubation (S1 and S2, Fig. 2A). Uptake removal in S1 and S2 followed the flow-force relationship (r^2 = 0.999), while uptake in the control (SC) followed a linear trend (r^2 = 0.997). Significantly high uptake rates were found in S1 and S2 compared with SC at 20 h (GLM-ANCOVA, F = 585.4, P<0.001); also, uptake rates were significantly different between S1 and S2 (GLM-ANCOVA, F = 199.7, P<0.001) (Fig. 2B). After 20 h of nitrate addition, the organisms were able to uptake phosphate down to low nanomolar threshold values within 5.5 h ($[P_e]_A$ = 5.6 and 7.7 nM phosphate, subsamples S1 and S2, respectively), while the [^{32}P] phosphate pulse applied to SC was still being removed (Fig. 2A). The maximum uptake rate activation during the experiments occurred at 39.17 h with up to a 25-fold increase (Fig. 4). The uptake rates among the [^{32}P] phosphate pulses applied after 39 h of nitrate addition were not statistically different when comparing S1 and S2 (GLM-ANCOVA: F = 2.8, P = 0.06), although highly significant if compared with the control SC (GLM-ANCOVA: F = 265.6, P<0.001). The time course of [^{32}P] phosphate removal showed the progressive increase in L_P, measured at 20 h and 39.17 h in comparison with the control (Figs 2 and 4).

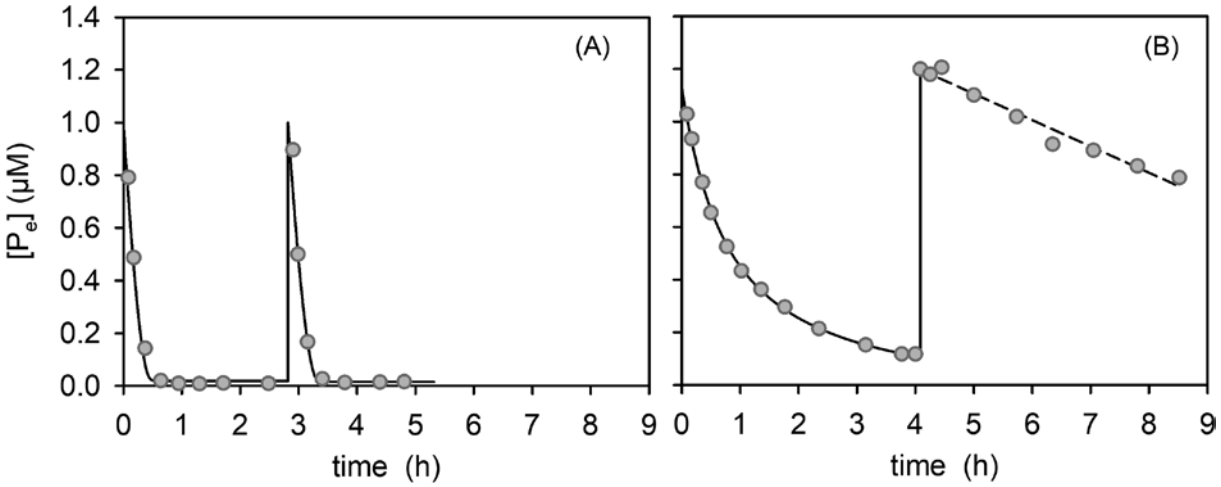

Figure 1. Comparison of the time course of [^{32}P] phosphate removal by phytoplankton in Lago Rodó (A) during groundwater supply (experiment A) and (B) after several months of groundwater discharge interruption (experiment B). The solid curves represent the best fit obtained with the flow-force equations (equations 1 and 2). The dashed line represents the linear regression fit. Kinetic parameters are shown in Table 3.

Table 3. Kinetic parameters of phosphate uptake by phytoplankton from Lago Rodó. Exp: experiment identification; Sbs: subsample (time of pulse addition); [^{32}P] pulse: initial [^{32}P] phosphate applied. Kinetic parameters of curve fitting of the Falkner's flow-force model; L_P and L: conductivity coefficients; $[P_e]_A$: threshold value; r^2: determination coefficient of the flow-force model fitting. *Kinetic parameters obtained with linear regression.

Exp	Sbs (h)	[^{32}P] pulse (µM)	L_P	L	$[P_e]_A$ (nM)	r^2
			µmol P_i (mg Chl *a* h)$^{-1}$			
A	S1	1.0	11.81	0.2	19.0	0.992
	S1	1.0	9.56	0.2	15.2	0.980
B	S1	1.2	1.22	0.1	62.9	0.999
	S1	1.2	0.79*	–	–	0.969
C	SC (20)	0.45	0.53*	–	–	0.997
	S1 (20)	0.45	0.76	0.6×10^{-3}	5.6	0.999
	S1 (39.17)	0.45	11.83	–	15.9	0.999
	S1 (40.17)	0.6	13.46	–	16.7	0.999
	S2 (20)	0.85	0.62	0.6×10^{-3}	7.7	0.999
	S2 (39.17)	0.85	11.74	–	12.6	0.999
	S2 (40.17)	0.6	15.13	–	22.2	0.999
D	SC (24)	0.85	0.41*	–	–	0.965
	S1 (24)	0.9	0.51	–	38.1	0.982
	S1 (47.92)	0.9	9.23	–	21.2	0.999
	S1 (49.08)	2.4	2.10	0.02	33.7	0.998
	S2 (24)	1.8	0.91	–	28.1	0.996
	S2 (47.92)	1.8	8.85	–	23.8	0.999
	S2 (49.08)	2.4	5.19	–	39.1	0.999

As regards experiment D, similar results to those in experiment C (Fig. 3A) were obtained with higher [^{32}P] phosphate concentrations. The maximum uptake rate increase was detected at 48 h (22-fold rate increase) (Fig. 4). After the following µM [^{32}P] phosphate pulses applied 1 h later, a 4-fold decrease in L_P was measured. The semilogarithmic replots in Figs 3B–D show that progressive uptake rates increase at 24 h and 47.92 h of nitrate preincubation and that L_P decreases after the next µM [^{32}P] phosphate pulses. The differences in uptake rates between S1 and S2 were significant in the first and third pulses (Fig. 3B; GLM-ANCOVA, $F = 100.0$, $P<0.001$; and Fig. 3D, $F = 22.8$, $P<0.001$) and non-significant in the second pulses (Fig. 3C). The uptake rates among the three [^{32}P] phosphate pulses within each subsample were also different (S1: GLM-ANCOVA, $F = 21.4$, $P<0.001$; S2: $F = 30.4$, $P<0.001$). Fig. 4 shows the changes in [^{32}P] phosphate uptake activity against incubation time and the corresponding treatments of experiments C and D.

DISCUSSION

This study reveals that the alleviation of N-deficiency triggers the activation of high-affinity phosphate uptake systems of bloom-forming cyanobacteria in order to sustain exponential growth. Cyanobacterial resilience under nutrient deficiency, and even bloom formation, may be ascribed to the rapid activation of nutrient uptake systems after short-term nutrient fluctuations. Within 24 h, an N-deficient cyanobacterial population that receives nitrate input re-establishes its active phosphate uptake and exponential growth. The appropriate physiological reaction time by organisms to transient availability of nutrients may determine the survival of populations (Aubriot and Bonilla 2012, 2018). The influence of shifting ambient N:P ratios on the phosphate uptake kinetics of phytoplankton dominated by *Planktothrix agardhii* has already been shown in Lago Rodó

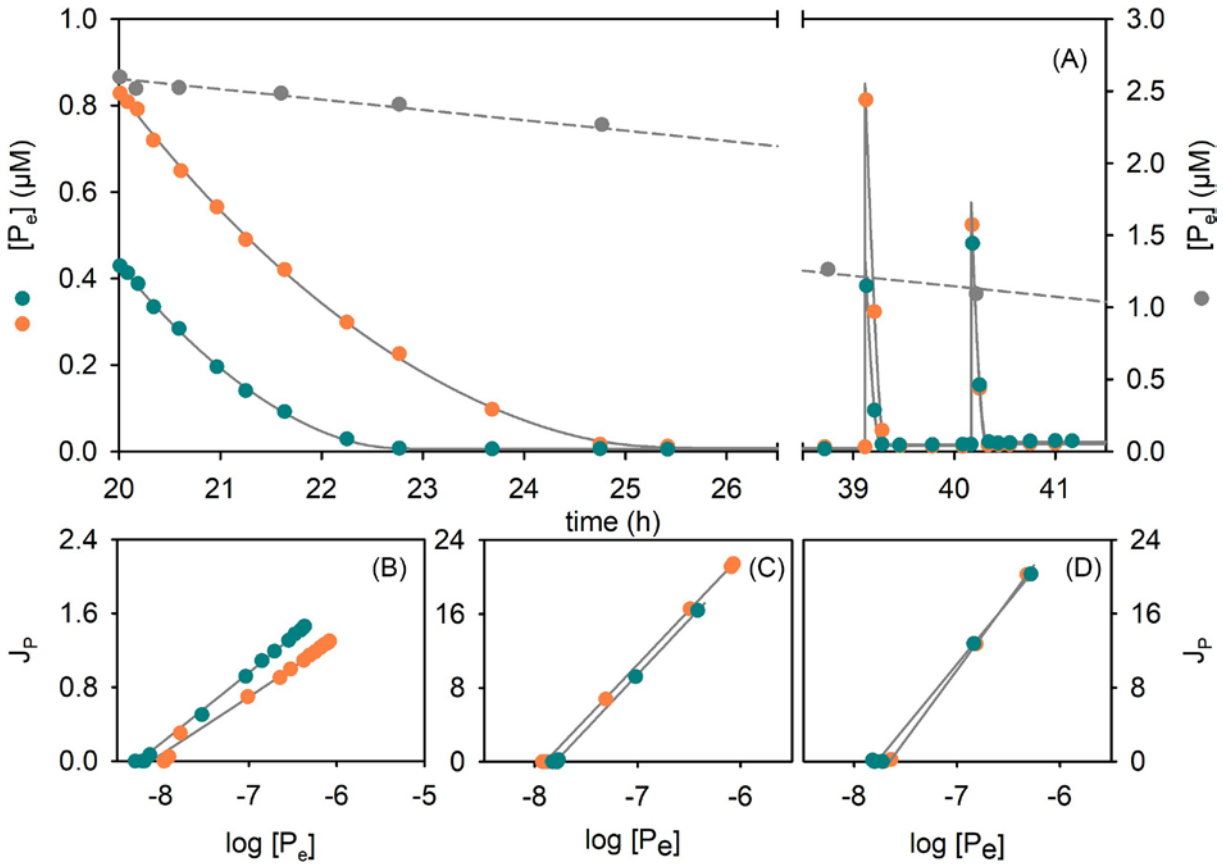

Figure 2. Time course of [^{32}P] phosphate removal by phytoplankton of Lago Rodó in experiment C. [^{32}P] phosphate removal was tested 20 h after nitrate preincubation (blue circles, subsample S1; orange circles, subsample S2). The control (SC) did not receive a nitrate input (gray circles). The initial [^{32}P] phosphate in SC was recalculated with equation 4. The solid curves represent the best fit obtained with the Falkner flow-force equation (equations 1 and 2). The dashed line represents the linear regression fit. Kinetic parameters are shown in Table 3. (B)–(D): Thellier plots of the concentration dependence of incorporation rates obtained from the time course of phosphate removal in S1 and S2 shown in (A). The uptake rate J_P is given in μmol Pi (mg Chl *a* h)$^{-1}$; the logarithm of the external phosphate concentration [P_e] is expressed relative to the unit standard concentration (1 M). (B) and (C): blue (S1) and orange (S2) circles correspond to 0.45 μM and 0.85 μM [^{32}P] phosphate pulses, respectively, applied at (B) 20 h and (C) 39.17 h of nitrate addition. (D): blue (S1) and orange circles (S2) correspond to 0.6 μM μM [^{32}P] phosphate pulses applied at 40.17 h of nitrate addition. Note the different scales in J_P between (B), (C) and (D).

(Aubriot and Bonilla 2018). In the present study, the cause-effect of N inputs on the regulation of affinity and activity of phosphate uptake systems of N-deficient cyanobacterial populations was demonstrated. Therefore, the control of N and P inputs into N-limited lakes with resilient non-N_2-fixing cyanobacterial populations is crucial to prevent the activation of high-affinity phosphate uptake systems and the rapid accumulation of polyphosphate reserves, which otherwise would stimulate increased growth rate.

This study demonstrates that the activation of phosphate uptake systems is facilitated by DIN supply in N-deficient non-N_2-fixing cyanobacterial populations. The reactivation of phosphate uptake systems occurred within 24 h after DIN input, and, based on the high uptake rates (L_P) determined here, the acquired phosphate needs to be immediately transformed into polyphosphate reserves in order to avoid cytoplasmic osmotic problems and phosphate leakage from the cells (Plaetzer *et al.* 2005). The high activation of phosphate uptake by up to 25-fold can be explained by a significant change in the cell membrane high-affinity P-binding proteins (Scanlan *et al.* 1997; Juntarajumnong *et al.* 2007; Kimura, Shiraiwa and Suzuki 2009). Changes in functional organization of membrane proteins in cyanobacteria occur via Pho regulon gene expression as a response to phosphate sufficient or deficient growth conditions (Suzuki *et al.* 2004; Schwarz and Forchhammer 2005; Juntarajumnong *et al.* 2007; Orchard, Webb and Dyhrman 2009; Pitt *et al.* 2010; Wang *et al.* 2018). Wang *et al.* (2018) postulated that N addition to a P-deficient *Dolichospermum* (N_2-fixing cyanobacterium) significantly upregulated *pstS* and *phoD* genes involved in P-transport and the hydrolysis of phosphomonoesters to overcome P-deficiency. Furthermore, N addition was shown to recover the ability of *Dolichospermum* to form polyphosphate bodies (Wang *et al.* 2018). This study shows the dynamics of this phenomenon extended to natural communities dominated by non-N_2-fixing cyanobacteria and the interaction with dissolved N, when nitrate supply initiates the activation of phosphate uptake. After the activation of phosphate uptake systems, organisms recover the capacity to adjust the uptake kinetics within minutes, which is in line with the timescale of phosphate fluctuations (Aubriot, Bonilla and Falkner 2011; Aubriot and Bonilla 2012; Amaral, Bonilla and Aubriot 2014). The recovery of phosphate uptake regulation capabilities is evident in experiment D when more than a 4-fold reduction in the uptake rate occurs from one phosphate pulse to the next. In light of the present results, it may be concluded that the time sequence of the regulatory uptake response also works in a flexible way. Therefore, cyanobacterial populations are able to activate and decelerate phosphate uptake as well as to increase and decrease

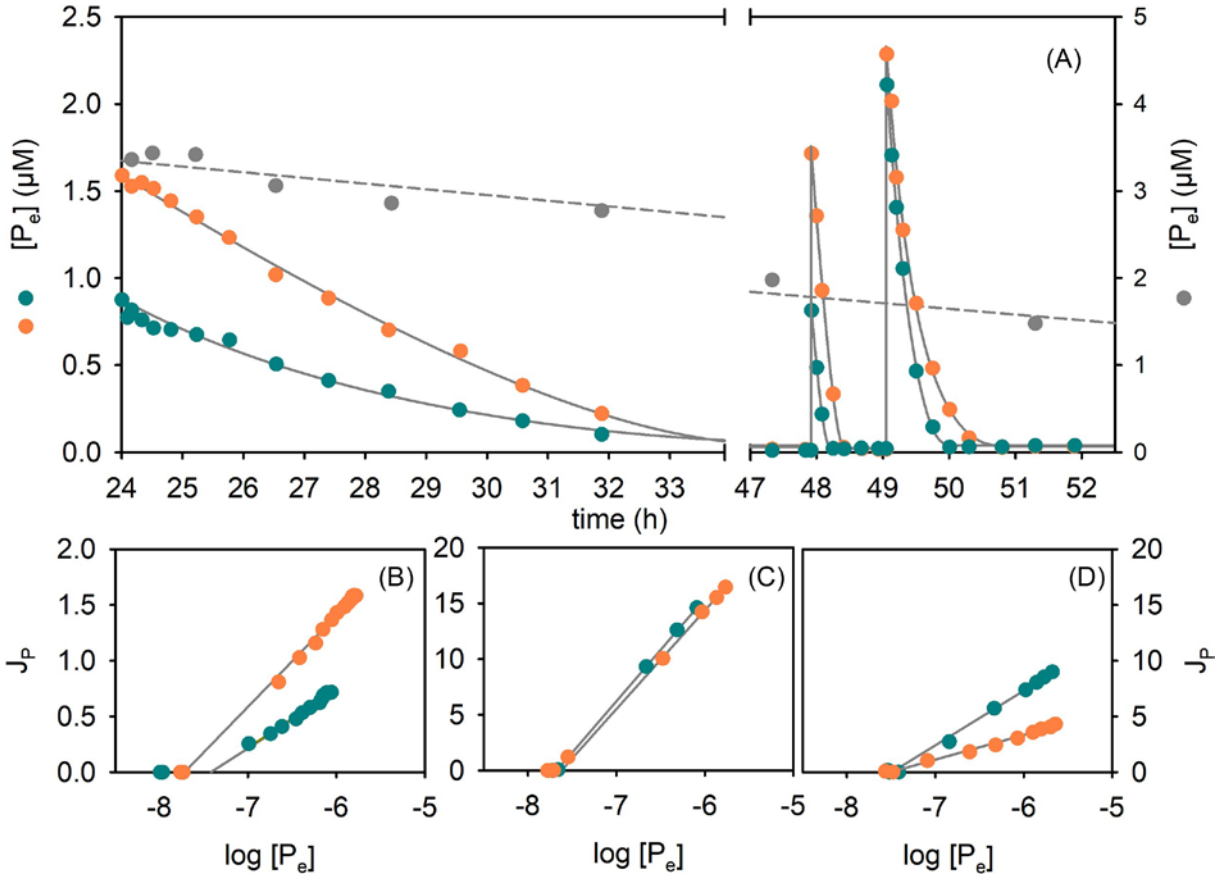

Figure 3. Time course of [^{32}P] phosphate removal by phytoplankton of Lago Rodó in experiment D. [^{32}P] phosphate removal was tested 24 h after nitrate preincubation (blue circles, subsample S1; orange circles, subsample S2). The control (SC) did not receive a nitrate input (gray circles). The initial [^{32}P] phosphate in SC was recalculated with equation 4. The solid curves represent the best fit obtained with the Falkner flow-force model (equations 1 and 2). The dashed line represents the linear regression fit. (B)–(D): Thellier plots of the concentration dependence of incorporation rates obtained from the time course of phosphate removal in S1 and S2 shown in (A). The uptake rate J_P is given in μmol Pi (mg Chl *a* h)$^{-1}$; the logarithm of the external phosphate concentration [P_e] is expressed relative to the unit standard concentration (1 M). (B) and (C): blue (S1) and orange (S2) circles correspond to 0.8 μM and 1.8 μM [^{32}P] phosphate pulses, respectively, applied at (B) 24 h and (C) 47.92 h of nitrate addition. (D): blue (S1) and orange circles (S2) correspond to 2.4 μM μM [^{32}P] phosphate pulses applied at 49.08 h of nitrate addition. Note the different scales in J_P between (B), (C) and (D). Kinetic parameters are shown in Table 3.

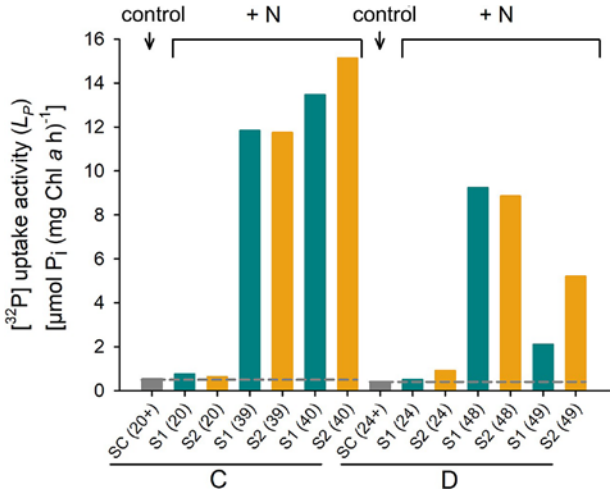

Figure 4. [^{32}P] phosphate uptake activity (L_P) as a function of treatments: control SC (gray bars, without nitrate input), S1 and S2 (with nitrate input, +N; blue and orange bars, respectively) in experiments C and D. The timing at which each L_P was determined is defined between brackets (h). Horizontal dashed lines indicate the level of L_P in control SC throughout the experiments.

nutrient affinity, from minutes to several hours (i.e. from kinetic regulation to membrane protein reconstruction), and according to the ongoing environmental N and P fluctuations in order to ensure population survival.

The whole process of phosphate uptake activation may occur within the time span of a bioassay (several days), in which adding N stimulates growth but adding both N and P results in higher cyanobacterial biomass after several days of incubation (Xu *et al.* 2010; Chislock, Sharp and Wilson 2014; Paerl *et al.* 2016; Aguilera *et al.* 2017). In the present experiments, the dominant cyanobacteria that grew with N and P additions were *P. agardhii* and *R. mediterranea*; however, no growth effect was noticed when only P was supplied. Considering that phosphate was relatively high in lake water (2.4 and 2.5 μM SRP), the addition of N alone would have resulted in similar growth responses as those found in S1 and S2 due to the activation of phosphate uptake systems. Generally, it is assumed that colimitation by N and P is biochemically independent (Saito, Goepfert and Ritt 2008). Nonetheless, the results presented here provide evidence that supports the hypothesis of a facilitating dependence of N on P acquisition (*sensu* Saito, Goepfert and Ritt 2008), concerning the N requirements of synthesizing N-rich P-transporters and phosphatases (Wang *et al.* 2018). The present results offer a physiological interpretation of the classical N, P and NP enrichment experiments,

in which N and P limitations may not occur simultaneously but partially overlapped in time. Moreover, adding N to the environment may not help to control cyanobacterial blooms (Chislock, Sharp and Wilson 2014) since N sufficiency allows high-affinity phosphate uptake systems to be functionally active and therefore ensure bloom persistence and development.

In urban areas, one important N source is atmospheric deposition, which cannot be locally controlled, and that was found to change phytoplankton nutrient limitations in lakes by shifting N:P ratios (Elser *et al.* 2009) and also bloom formation (Zhan *et al.* 2017). However, the timescale in which such N:P shifts affect phytoplankton physiology remains unknown at present. The concentration of nitrate used in this study is within the concentration range of atmospheric nitrogen deposition found in residential and crop areas (Yang *et al.* 2010). Therefore, the nitrate inputs used here can be representative of short-term events of direct rainwater in combination with catchment runoff (Seitzinger *et al.* 2010). Moreover, global predictions for future N loading in freshwater systems maintain that changes in the precipitation regime due to climate change will result in a significant increase in total N loading in freshwaters, thereby promoting eutrophication (Sinha, Michalak and Balaji 2017). Therefore, strong efforts to reduce loads of N and P in lakes should be undertaken to effectively control cyanobacterial growth (Davis *et al.* 2015; Paerl *et al.* 2016). The reaction timescale of cyanobacterial populations to N inputs shown here and their capability to shift to active removal of available phosphate reveal the physiological basis of bloom formation and concern about processes usually overlooked in statistically based predictive models.

This study shows that within 24 h of N-deficiency alleviation in bloom-forming cyanobacterial populations, high-affinity phosphate uptake systems are activated. Uptake activation permits organisms to acquire the necessary cellular P reserves to sustain constant growth. Additionally, the rapid and flexible physiological response allows non-N_2- fixing cyanobacteria to survive and even bloom during periods of low nutrient concentrations, particularly when N recycling produces stochastic DIN inputs which, in turn, allows populations to exploit the available phosphate. Therefore, the reduction of DIN availability also needs to be considered to control non-N_2- fixing cyanobacteria in order to prevent the activation of high-affinity phosphate uptake systems. This short-term process of phosphate uptake activation and the rapid phosphate removal hinders proper detection by conventional analytical methods and classical monitoring programs of lakes, therefore challenging lake-restoring programs and bloom predictions.

ACKNOWLEDGMENTS

The author is grateful to Leticia Vidal and Mauricio González-Piana for the microscopic identification and counting, and also to Sylvia Bonilla for her useful comments on this manuscript. I am grateful to the anonymous reviewers who helped to improve the manuscript with detailed comments and relevant suggestions.

FUNDING

This work was supported by the Basic Science Development Program (PEDECIBA), University Commission for Scientific Research (CSIC), Clemente Estable Fund (Project: FCE 7026) and National Agency for Research and Innovation (Project: ANII FCE2009 _2330).

Conflict of interest. None declared.

REFERENCES

Aguilera A, Aubriot L, Echenique RO *et al.* Synergistic effects of nutrients and light favor Nostocales over non-heterocystous cyanobacteria. *Hydrobiologia* 2017;**794**:241–55.

Amaral V, Bonilla S, Aubriot L. Growth optimization of the invasive cyanobacterium *Cylindrospermopsis raciborskii* in response to phosphate fluctuations. *Eur J Phycol* 2014;**49**:134–41.

Aubriot L, Bonilla S. Rapid regulation of phosphate uptake in freshwater cyanobacterial blooms. *Aquat Microb Ecol* 2012;**67**:251–63.

Aubriot L, Bonilla S. Regulation of phosphate uptake reveals cyanobacterial bloom resilience to shifting N:P ratios. *Freshw Biol* 2018;**63**:318–29.

Aubriot L, Wagner F, Falkner G. The phosphate uptake behaviour of phytoplankton communities in eutrophic lakes reflects alterations in the phosphate supply. *Eur J Phycol* 2000;**35**:255–62.

Aubriot L, Bonilla S, Falkner G. Adaptive phosphate uptake behaviour of phytoplankton to environmental phosphate fluctuations. *FEMS Microbiol Ecol* 2011;**77**:1–16.

Bonachela JA, Raghib M, Levin SA. Dynamic model of flexible phytoplankton nutrient uptake. *Proc Natl Acad Sci* 2011;**108**:20633–38.

Bormans M, Maršálek B, Jančula D. Controlling internal phosphorus loading in lakes by physical methods to reduce cyanobacterial blooms: A review. *Aquat Ecol* 2016;**50**:407–22.

Chaffin JD, Davis TW, Smith DJ *et al.* Interactions between nitrogen form, loading rate, and light intensity on *Microcystis* and *Planktothrix* growth and microcystin production. *Harmful Algae* 2018;**73**:84–97.

Chislock MF, Sharp KL, Wilson AE. *Cylindrospermopsis raciborskii* dominates under very low and high nitrogen-to-phosphorus ratios. *Water Res* 2014;**49**:207–14.

Davis TW, Bullerjahn GS, Tuttle T *et al.* Effects of increasing nitrogen and phosphorus concentrations on phytoplankton community growth and toxicity during *Planktothrix* blooms in Sandusky Bay, Lake Erie. *Environ Sci Technol* 2015;**49**:7197–207.

Dokulil M, Teubner K. Cyanobacterial dominance in lakes. *Hydrobiologia* 2000;**438**:1–12.

Dolman AM, Rücker J, Pick FR *et al.* Cyanobacteria and cyanotoxins: The influence of nitrogen versus phosphorus. *PLoS One* 2012;**7**:e38757.

Elser JJ, Andersen T, Baron JS *et al.* Shifts in lake N:P stoichiometry and nutrient limitation driven by atmospheric nitrogen deposition. *Science* 2009;**326**:835–37.

Falkner G, Falkner R. Phosphate uptake by eukaryotic algae in cultures and by a mixed phytoplankton population in a lake: Analysis by a flow force relationship. *Botanica Acta* 1989;**102**:283–89.

Falkner G, Falkner R, Schwab A. Bioenergetic characterization of transient state phosphate uptake by the cyanobacterium *Anacystis nidulans*. *Arch Microbiol* 1989;**152**:353–61.

Falkner G, Wagner F, Small JV *et al.* Influence of fluctuating phosphate supply on the regulation of phosphate uptake by the blue-green alga *Anacystis nidulans*. *J Phycol* 1995;**31**:745–53.

Falkner R, Priewasser M, Falkner G. Information processing by cyanobacteria during adaptation to environmental phosphate fluctuations. *Plant Sign Behav* 2006;**1**:212–20.

Galloway JN, Dentener FJ, Capone DG *et al.* Nitrogen cycles: Past, present, and future. *Biogeochemistry* 2004;**70**:153–226.

Guillard R. Counting slides. In: Sournia A (ed.) *Phytoplankton manual*. Paris: Unesco, 1978;182–90.

Hillebrand H, Dürselen C, Kirschtel D *et al.* Biovolume calculation for pelagic and benthic microalgae. *J Phycol* 1999;**35**:403–24.

Istvánovics V, Pettersson K, Don P *et al.* Evaluation of phosphorus deficiency indicators for summer phytoplankton in Lake Erken. *Limnol Oceanogr* 1992;**37**:890–900.

Juntarajumnong W, Hirani T, Simpson J *et al.* Phosphate sensing in *Synechocystis* sp. PCC 6803: SphU and the SphS-SphR two-component regulatory system. *Arch Microbiol* 2007;**188**:389–402.

Kimura S, Shiraiwa Y, Suzuki I. Function of the N-terminal region of the phosphate-sensing histidine kinase, SphS, in *Synechocystis* sp. PCC 6803. *Microbiology* 2009;**155**:2256–64.

Komárek J, Anagnostidis K. *Cyanoprokaryota II. Teil Oscillatoriales*. München: Spektrum Akademischer Verlag, 2005.

Lean DRS, Pick FR. Photosynthetic response of lake plankton to nutrient enrichment: A test for nutrient limitation. *Limnol Oceanogr* 1981;**26**:1001–19.

Lürling M, Waajen G, de Senerpont Domis LN. Evaluation of several end-of-pipe measures proposed to control cyanobacteria. *Aquat Ecol* 2016;**50**:499–519.

Nusch E. Comparisons of different methods for chlorophyll and phaeopigments determination. *Arch Hydrobiol Beih Ergebn Limnol* 1980;**14**:14–36.

Orchard ED, Webb EA, Dyhrman ST. Molecular analysis of the phosphorus starvation response in *Trichodesmium* spp. *Environ Microbiol* 2009;**11**:2400–11.

Paerl H. Mitigating toxic planktonic cyanobacterial blooms in aquatic ecosystems facing increasing anthropogenic and climatic pressures. *Toxins* 2018;**10**:76.

Paerl HW, Scott JT, McCarthy MJ *et al.* It takes two to tango: When and where dual nutrient (N & P) reductions are needed to protect lakes and downstream ecosystems. *Environ Sci Technol* 2016;**50**:10805–13.

Paerl HW, Xu H, Hall NS *et al.* Controlling cyanobacterial blooms in hypertrophic Lake Taihu, China: Will nitrogen reductions cause replacement of non-N_2 fixing by N_2 fixing taxa? *PLoS One* 2014;**9**:e113123.

Pitt FD, Mazard S, Humphreys L *et al.* Functional characterization of *Synechocystis* sp. strain PCC 6803 pst1 and pst2 gene clusters reveals a novel strategy for phosphate uptake in a freshwater cyanobacterium. *J Bacteriol* 2010;**192**:3512–23.

Plaetzer K, Thomas SR, Falkner R *et al.* The microbial experience of environmental phosphate fluctuations. An essay on the possibility of putting intentions into cell biochemistry. *J Theor Biol* 2005;**235**:540–54.

Roy E, Nguyen N, Bargu S *et al.* Internal loading of phosphorus from sediments of Lake Pontchartrain (Louisiana, USA) with implications for eutrophication. *Hydrobiologia* 2012;**684**:69–82.

Saito MA, Goepfert TJ, Ritt JT. Some thoughts on the concept of colimitation: Three definitions and the importance of bioavailability. *Limnol Oceanogr* 2008;**53**:276–90.

Sant'Anna CL. *Chlorococcales (Chlorophyceae) do Estado de Sao Paulo, Brasil*. Vaduz. F. Cramer, 1984.

Scanlan DJ, Silman NJ, Donald KM *et al.* An immunological approach to detect phosphate stress in populations and single cells of photosynthetic picoplankton. *Appl Environ Microbiol* 1997;**63**:2411–20.

Schindler DW. Evolution of phosphorus limitation in lakes. *Science* 1977;**195**:260–62.

Schindler DW, Hecky RE, Findlay DL *et al.* Eutrophication of lakes cannot be controlled by reducing nitrogen input: results of a 37-year whole-ecosystem experiment. *Proc Natl Acad Sci U S A* 2008;**105**:11254–58.

Schwarz R, Forchhammer K. Acclimation of unicellular cyanobacteria to macronutrient deficiency: Emergence of a complex network of cellular responses. *Microbiology* 2005;**151**:2503–14.

Seitzinger SP, Mayorga E, Bouwman AF *et al.* Global river nutrient export: A scenario analysis of past and future trends. *Global Biogeochem Cycles* 2010;**24**:GB0A08.

Sinha E, Michalak AM, Balaji V. Eutrophication will increase during the 21st century as a result of precipitation changes. *Science* 2017;**357**:405–08.

Smith VH, Schindler DW. Eutrophication science: Where do we go from here? *Trends Ecol Evol* 2009;**24**:201–07.

Sommaruga R, Robarts RD. The significance of autotrophic and heterotrophic picoplankton in hypertrophic ecosystems. *FEMS Microbiol Ecol* 1997;**24**:187–200.

Stomp M, van Dijk MA, van Overzee HMJ *et al.* The timescale of phenotypic plasticity and its impact on competition in fluctuating environments. *Am Nat* 2008;**172**:E169–E85.

Strickland JDH, Parsons TR. *A practical handbook of seawater analysis*. Ottawa: Fisheries Research Board, 1972.

Suzuki S, Ferjani A, Suzuki I *et al.* The SphS-SphR two component system is the exclusive sensor for the induction of gene expression in response to phosphate limitation in *Synechocystis*. *J Biol Chem* 2004;**279**:13234–40.

Thellier M. An electrokinetic interpretation of the functioning of biological systems and its application to the study of mineral salt absorption. *Ann Bot* 1970;**34**:983–1009.

Valderrama JC. The simultaneous analysis of total nitrogen and total phosphorus in natural waters. *Mar Chem* 1981;**10**:109–22.

Wagner F, Falkner R, Falkner G. Information about previous phosphate fluctuations is stored via an adaptive response of the high-affinity phosphate uptake system of the cyanobacterium *Anacystis nidulans*. *Planta* 1995;**197**:147–55.

Wang S, Xiao J, Wan L *et al.* Mutual dependence of nitrogen and phosphorus as key nutrient elements: One facilitates *Dolichospermum flos-aquae* to overcome the limitations of the other. *Environ Sci Technol* 2018;**52**:5653–61.

Wehr JD, Sheath RG. *Freshwater algae of North America. Ecology and classification*. Amsterdam: Academic Press, 2003.

Wu Z, Zeng B, Li R *et al.* Physiological regulation of *Cylindrospermopsis raciborskii* (Nostocales, Cyanobacteria) in response to inorganic phosphorus limitation. *Harmful Algae* 2012;**15**:53–58.

Xu H, Paerl HW, Qin B *et al.* Nitrogen and phosphorus inputs control phytoplankton growth in eutrophic Lake Taihu, China. *Limnol Oceanogr* 2010;**55**:420–32.

Yan X, Xu X, Wang M *et al.* Climate warming and cyanobacteria blooms: Looks at their relationships from a new perspective. *Water Res* 2017;**125**:449–57.

Yang R, Hayashi K, Zhu B *et al.* Atmospheric NH_3 and NO_2 concentration and nitrogen deposition in an agricultural catchment of Eastern China. *Sci Total Environ* 2010;**408**:4624–32.

Zhan X, Bo Y, Zhou F *et al.* Evidence for the importance of atmospheric nitrogen deposition to eutrophic Lake Dianchi, China. *Environ Sci Technol* 2017;**51**:6699–708.